Fast Continuous Swimming of Two Pelagic Predators, Saithe (Pollachius Virens) and Mackerel (Scomber Scombrus)

Videler, JJ; Hess, F

Published in:
Journal of Experimental Biology

Publication date:
1984

J. exp. Biol. **109**, 229–251 (1984)
Printed in Great Britain © *The Company of Biologists Limited 1984*

FAST CONTINUOUS SWIMMING OF SAITHE (*POLLACHIUS VIRENS*): A DYNAMIC ANALYSIS OF BENDING MOMENTS AND MUSCLE POWER

BY F. HESS AND J. J. VIDELER

Department of Zoology, State University Groningen, P.O. Box 14, 9750 AA Haren, The Netherlands

Accepted 7 October 1983

SUMMARY

This paper deals with the hydrodynamics and internal dynamics of fish swimming. Our analysis starts from kinematic data obtained for fast swimming saithe, and treats the fish as a flexible elongated body. The distribution along the body of the lateral bending moment and the bending power generated inside the fish are computed as well as the power spent on the water. The computed thrust implies a drag coefficient (based on wetted surface area) of about 0·007, which is probably an over-estimate. Our major result is that the bending moment does not travel as a running wave from head to tail like the lateral body curvature does, but behaves as a standing wave. The left and right sides produce alternate contractions simultaneously over the whole body length. This finding is in agreement with myographic data from the literature.

INTRODUCTION

In the preceding paper we presented a kinematic analysis of the swimming movements of saithe and mackerel (Videler & Hess, 1984). The present paper continues with a dynamic analysis, using the kinematic results of the first paper as a point of departure. This analysis is aimed at the hydrodynamic forces between fish and water, the bending moments inside a fish and the mechanical work done by the fish body during swimming.

We shall use Lighthill's (1960) hydrodynamic slender-body (or elongated-body) theory. The fish is assumed to be a streamlined body, ending in a vertical trailing edge of the tail fin. The water flows smoothly along the body surface and the stream lines leave the body at the trailing edge only. Viscous effects are ignored. Slender-body theory requires that the transverse dimensions of the body are small compared to its length and that the cross-section shape varies only gradually along the body in a lengthwise direction, and is therefore not applicable for mackerel. The tail fin of mackerel shows a sharp increase in height from the caudal peduncle onward (see Fig. 1 of Videler & Hess, 1984), whereas in saithe this increase is less abrupt, although still considerable. To what extent slender-body theory is applicable to swimming saithe will be discussed in a later section.

Key words: Fish, swimming, hydrodynamics, fish muscles.

The validity of Lighthill's (1960) theory is restricted to lateral oscillations of the fish body with an amplitude small in comparison to the body length. Although several more refined versions of slender-body theory have been developed (e.g. Lighthill, 1971, for large amplitude motions, Newman & Wu, 1972, for interaction between fins and body), the 1960 theory has the advantage of being relatively simple, and linear. The linearity is essential to our approach, because we represent the periodic lateral motion of the fish as a sum of several Fourier terms. Linearity implies that if a certain lateral motion is considered as the sum of two other motions, A and B say, then the lateral hydrodynamic force distribution belonging to it is obtained by summing the force distributions belonging to the motions A and B. Similarly for the lateral bending moments inside the fish.

The theoretical model presented in the next sections will be applied to the swimming movements of saithe as analysed in Videler & Hess (1984) from 13 film sequences.

MATHEMATICAL MODEL

We assume that the fish, to a good approximation, swims along a straight line at a constant speed. Our moving coordinate system is chosen such that the fish stays close to the x-axis and occupies a region between $x = 0$ (nose) and $x = L$ (tail). With respect to the coordinate frame the fluid has a uniform velocity U in the x-direction (Fig. 1). The z-axis points in the lateral direction, and the y-axis downward.

The 'centreline' (physically: the backbone) of the fish is described by the equation:

$$z = h(x,t),\ 0 \leqslant x \leqslant L\,. \tag{1}$$

We make the assumption that the fish is slender, which implies that its thickness and height are much smaller than its length L, also that $|h(x,t)| << L$ and that the angle between centreline and x-axis is small. In the following analysis we will treat the fish as a thin flexible rod under the influence of hydrodynamic forces. We consider only

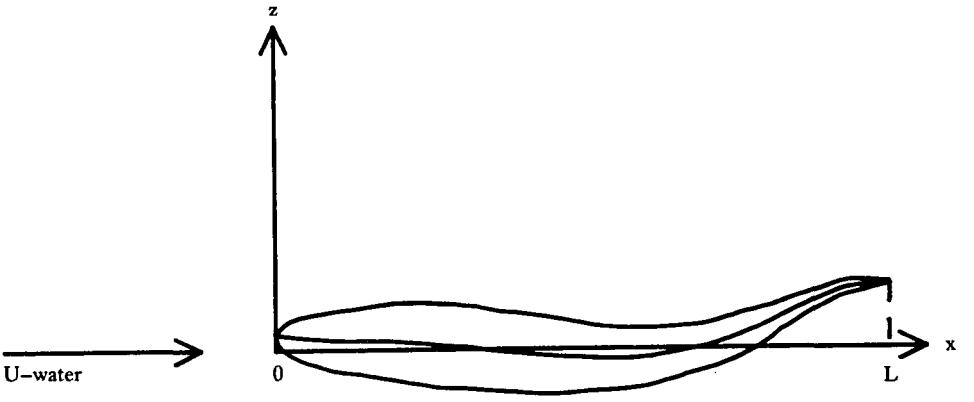

Fig. 1. Schematic dorsal view of fish and coordinate system.

lateral bending, because it appears to determine completely the variations in body shape of a swimming fish with the exception of the tail region and extended fins. For fast-swimming saithe this approach seems to be justified.

Let us look at the forces and moments acting on an arbitrary thin slab of the fish perpendicular to its backbone (Fig. 2). The slab lies between x and $x + \delta x$ and has length δx. The forces and moments experienced by the slab come from three regions: the anterior part of the body, the posterior part of the body and the water adjacent to the slab. We call the lateral force in the z-direction exerted at any section x by the anterior part on the posterior part $F(x)$. Hence the opposite force exerted by the posterior part on the anterior part is $-F(x)$. The moment exerted by the anterior part attempting to turn the posterior part counter-clockwise is called $M(x)$. Hence the opposite moment exerted by the posterior on the anterior is $-M(x)$. The lateral force exerted by the water per unit of length is $L(x)$. Thus the following lateral forces act on the slab:

$$F(x,t) - F(x + \delta x,t) + L(x,t)\delta x\,. \tag{2}$$

The moments acting on the slab are those from the anterior and posterior parts as well as the moment resulting from the pair of lateral forces acting a distance δx apart:

$$M(x,t) - M(x + \delta x,t) - F(x,t)\delta x\,. \tag{3}$$

The variable t is included as all quantities are time dependent. If δx is small enough we can replace $F(x + \delta x,t)$ by $F(x,t) + [\partial F(x,t)/\partial x]\delta x$ and $M(x + \delta x,t)$ analogously.

The total net force acting on the slab must equal the slab's mass times its lateral acceleration. Let the fish's body mass per unit length be $m_b(x)$. We then obtain:

$$-\frac{\partial F(x,t)}{\partial x} + L(x,t) = m_b(x)\frac{\partial^2 h(x,t)}{\partial t^2}\,, \tag{4}$$

where we dropped the common factor δx in all terms. The total net moment acting on the slab must equal its angular acceleration times the slab's moment of inertia about its vertical axis. This last quantity is negligibly small for a thin rod, therefore:

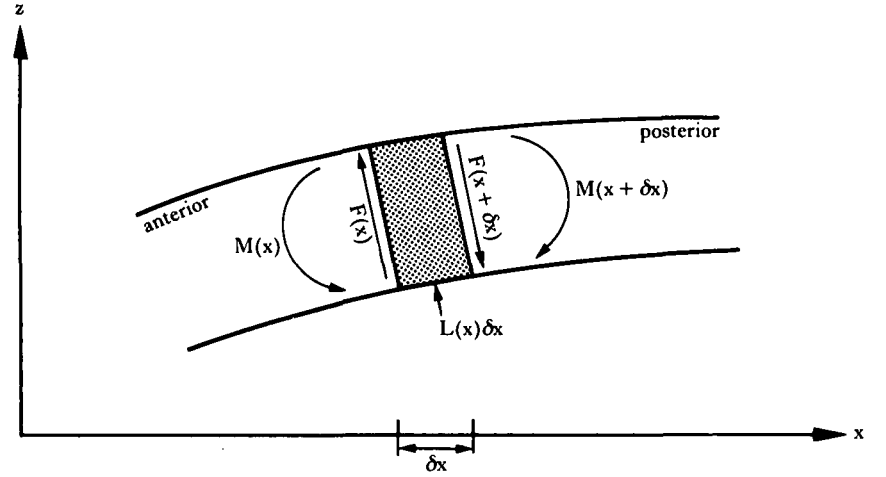

Fig. 2. Forces and moments acting on a thin slab of fish.

$$-\frac{\partial M(x,t)}{\partial x} - F(x,t) = 0. \tag{5}$$

The 'internal' force F and moment M vanish at the nose and tail ends:

$$\left.\begin{aligned} F(0,t) = F(L,t) &= 0, \\ M(0,t) = M(L,t) &= 0. \end{aligned}\right\} \tag{6}$$

These end conditions apply whenever the fish moves freely in the water. They would be violated if the fish were attached to some object at either its nose or its tail.

Equation (5) indicates that $F = -\partial M/\partial x$. Substitution into (4) yields:

$$\frac{\partial^2 M(x,t)}{\partial x^2} = m_b(x)\frac{\partial^2 h(x,t)}{\partial t^2} - L(x,t). \tag{7}$$

For L(x,t), the hydrodynamic lateral force per unit length, we take the following expression, as derived by Lighthill (1960) for his small-amplitude slender-body theory:

$$-L(x,t) = \left(\frac{\partial}{\partial t} + U\frac{\partial}{\partial x}\right)\left\{m_a(x)\left(\frac{\partial}{\partial t} + U\frac{\partial}{\partial x}\right)h(x,t)\right\}, \tag{8}$$

where $m_a(x)$ is the lateral added mass per unit length and it depends on the local cross-section shape of the fish. The combination of (7) and (8) gives an equation connecting h(x,t) with the bending moment M(x,t). If the lateral motion h(x,t) is given, together with L, U, $m_a(x)$ and $m_b(x)$, then the second derivative of the bending moment $\partial^2 M/\partial x^2$, can be obtained and from this follows M(x,t) itself after integrating twice. However, note that whereas we must satisfy four end conditions (6), we can only adjust two integration constants. Hence, for an arbitrary lateral motion, at most two of the four end conditions can be satisfied. This means that only a restricted class of lateral motions h(x,t) is allowed. This restriction is equivalent to the restriction imposed by the recoil conditions stated by Lighthill (1960).

It should be pointed out that essentially the same mathematical model was outlined by Wu (1971), who explicitly took elasticity into account and also by Lighthill (private communication in 1978), who treated the fish as an elastic beam. In this paper we do not distinguish between the elastic bending moments and the bending moments generated by the fish's muscles.

Let us now consider the mechanical energy generated and spent by a thin slab at an arbitrary section of the fish. As we are interested in the muscle power required to propel the fish by bending its body, we will first look at the power (= energy per unit time) exerted by the bending moment M(x,t). The mechanical power produced inside the slab between x and $x + \delta x$ equals the bending moment times the rate of change of the slab's curvature:

$$M(x,t)\frac{\partial}{\partial t}\frac{\partial^2 h(x,t)}{\partial x^2}\delta x. \tag{9}$$

Hence, the power produced per unit length equals:

$$P_1(x,t) = M(x,t)\frac{\partial}{\partial t}\frac{\partial^2 h(x,t)}{\partial x^2}. \tag{10}$$

How is this power spent? Firstly, some power is spent on the slab itself by increasing its kinetic energy:

$$\frac{\partial}{\partial t}\left\{\tfrac{1}{2}m_b(x)\,\delta x\left[\frac{\partial h(x,t)}{\partial t}\right]^2\right\} = m_b(x)\delta x\frac{\partial h(x,t)}{\partial t}\frac{\partial^2 h(x,t)}{\partial t^2}. \tag{11}$$

Secondly, the power spent on the water adjacent to the slab equals (force times velocity):

$$-L(x,t)\,\delta x\frac{\partial h(x,t)}{\partial t}. \tag{12}$$

These two parts, by virtue of (4), add up to

$$-\frac{\partial F(x,t)}{\partial x}\frac{\partial h(x,t)}{\partial t}\delta x. \tag{13}$$

Hence, the power spent per unit length on fish plus water equals:

$$P_2(x,t) = \frac{\partial^2 M(x,t)}{\partial x^2}\frac{\partial h(x,t)}{\partial t} \tag{14}$$

where we used (5). The difference $\{P_1(x,t)-P_2(x,t)\}\delta x$ is the power 'exported' by the slab to the anterior and posterior parts of the fish. At each instant, t, the power generated in the whole fish must equal the power spent on the whole fish plus water:

$$\int_0^L P_1(x,t)\,dx = \int_0^L P_2(x,t)\,dx = P(t). \tag{15}$$

For the difference P_1-P_2 we have:

$$\begin{aligned} P_1(x,t) - P_2(x,t) &= M(x,t)\frac{\partial}{\partial t}\frac{\partial^2 h(x,t)}{\partial x^2} - \frac{\partial^2 M(x,t)}{\partial x^2}\frac{\partial h(x,t)}{\partial t} \\ &= \frac{\partial R(x,t)}{\partial x}, \end{aligned} \tag{16}$$

where the function R is defined by:

$$R(x,t) = M(x,t)\frac{\partial}{\partial t}\frac{\partial h(x,t)}{\partial x} - \frac{\partial M(x,t)}{\partial x}\frac{\partial h(x,t)}{\partial t}. \tag{17}$$

R(x,t) is the power transported inside the fish across the section at x from anterior to posterior. The first term in the right-hand side of (17) is the power exerted by the anterior part on the posterior part by moment and angular velocity, the second term is the power exerted by the anterior part on the posterior part by force and lateral velocity. From (16) it follows:

$$\int_0^{x_0}\{P_1(x,t) - P_2(x,t)\}dx = R(x_0,t). \tag{18}$$

If L is substituted for x_0, then (15) shows that R(L,t) must vanish. This agrees with the end conditions (6): both M and $\partial M/\partial x$ vanish at $x = L$ and hence R according to (17).

In addition to the power transported inside the fish, as represented by R, there is also power leaving the fish body and entering adjacent water at some places and

returning to the body elsewhere. The power spent on the water per unit length is given by (12). Hence, the power transport outside the fish across the plane $x = x_0$ is:

$$R_w(x_0) = \int_0^{x_0} -L(x,t)\frac{\partial h(x,t)}{\partial t}\,dx. \tag{19}$$

Periodic motion

We now apply the theory of the previous section to the periodic swimming motion as described by Videler & Hess (1984). The time period of the lateral motion is T, and h(x,t) is represented by a Fourier series:

$$h(x,t) = \sum_{\substack{j=1\\ \text{odd}}}^{5} \{a_j(x)\cos j\omega t + b_j(x)\sin j\omega t\},\ \omega = 2\pi/T, \tag{20}$$

which can be written in the alternative form:

$$h(x,t) = \sum_{j=1,3,5} h_j(x)\cos j\omega[t - \tau_j(x)], \tag{21}$$

where the $h_j(x)$ are amplitude functions and the $\tau_j(x)$ phase functions. The time origin is chosen such that $\tau_1(L) = 0$ by definition.

We define the function f by:

$$f(x,t) = \frac{\partial^2 h(x,t)}{\partial x^2}. \tag{22}$$

It is the lateral body curvature function, which we can write as:

$$f(x,t) = \sum_{j=1,3,5} \{a_j''(x)\cos j\omega t + b_j''(x)\sin j\omega t\}$$

$$= \sum_{j=1,3,5} f_j(x)\cos j\omega[t - \sigma_j(x)]. \tag{23}$$

The Fourier coefficients $a_j(x)$ and $b_j(x)$ are represented by cubic splines are explained by Videler & Hess (1984). We have chosen the end conditions of vanishing curvature at both nose and tail: $f(0,t) = f(L,t) = 0$. The numerical values for $a_j''(x)$ and $b_j''(x)$ are obtained by the 'spline-on-spline' method.

Let us represent the lateral bending moment M by:

$$M(x,t) = \sum_{j=1,3,5} \{p_j(x)\cos j\omega t + q_j(s)\sin j\omega t\}$$

$$= \sum_{j=1,3,5} M_j(x)\cos j\omega[t - \mu_j(x)]. \tag{24}$$

The $p_j(x)$ and $q_j(x)$ are Fourier coefficients, the $M_j(x)$ amplitude functions and the $\mu_j(x)$ phase functions.

If we substitute (24) and (20) for M(x,t) and h(x,t) in equations (7) and (8) we obtain a set of equations relating the Fourier coefficients $a_j(x)$, $b_j(x)$ and $p_j(x)$, $q_j(x)$. Each of the frequencies (j = 1,3,5) can be dealt with separately. After carrying out the necessary differentiations, we obtain:

$$\left.\begin{aligned} p_j''(x) &= -j^2\omega^2\{m_a(x)+m_b(x)\}a_j(x) + U_j\omega\{2m_a(x)b_j'(x) + m_a'(x)b_j(x)\} \\ &\quad + U^2\{m_a(x)a_j''(x) + m_a'(x)a_j'(x)\} \\ q_j''(x) &= -j^2\omega^2\{m_a(x)+m_b(x)\}b_j(x) - Uj\omega\{2m_a(x)a_j'(x) + m_a'(x)a_j(x)\} \\ &\quad + U^2\{m_a(x)b_j''(x) + m_a'(x)b_j'(x)\}. \end{aligned}\right\} \quad (25)$$

Integrating twice yields $p_j(x)$ and $q_j(x)$, which determine the contribution of the jth frequency to the bending moment. However, the correct solution requires that both M and M′ vanish at the end points, hence that:

$$\left.\begin{aligned} p_j'(x) = q_j'(x) = 0 \\ p_j(x) = q_j(x) = 0 \end{aligned}\right\} \text{ for } x = 0 \text{ and } x = L,\ j = 1,3,5. \quad (26)$$

These 'recoil-conditions' will not automatically be satisfied. The next section gives a method to deal with this problem.

Values for $P_1(x,t)$, $P_2(x,t)$, $R(x,t)$, etc. are obtained by substitution of the expressions (20) and (24) and their derivatives. The mean bending power per unit length is:

$$\bar{P}_1(x) = \tfrac{1}{2}\sum_{j=1,3,5} j\omega\{p_j(x)b_j''(x) - q_j(x)a_j''(x)\}. \quad (27)$$

The mean power spent per unit length on fish plus water is:

$$\bar{P}_2(x) = \tfrac{1}{2}\sum_{j=1,3,5} j\omega\{p_j''(x)b_j(x) - q_j''(x)a_j(x)\} \quad (28)$$

and the mean internal power transport is:

$$\bar{R}(x) = \tfrac{1}{2}\sum_{j=1,3,5} j\omega\{p_j(x)b_j'(x) - q_j(x)a_j'(x) - p_j'(x)b_j(x) + q_j'(x)a_j(x)\}. \quad (29)$$

According to Lighthill (1960) the mean thrust $\bar{\theta}$ for a periodic motion is given by:

$$\bar{\theta} = \tfrac{1}{2}m_a(L)\left\{\overline{\left[\frac{\partial h(x,t)}{\partial t}\right]^2} - U^2\overline{\left[\frac{\partial h(x,t)}{\partial x}\right]^2}\right\}\Big|_{x=L} \quad (30)$$

and the mean power delivered by the fish:

$$\bar{P} = Um_a(L)\left\{\overline{\left[\frac{\partial h(x,t)}{\partial t}\right]^2} + U\overline{\frac{\partial h(x,t)}{\partial t}\,\frac{\partial h(x,t)}{\partial x}}\right\}\Big|_{x=L} \quad (31)$$

Both $\bar{\theta}$ and $\bar{P}$ depend only on what happens at the tail end. The hydrodynamic Froude efficiency is given by:

$$\eta = \bar{\theta}U/\bar{P}. \quad (32)$$

If the lateral motion has the form (20), then we have:

$$\bar{\theta} = \tfrac{1}{4}m_a(L)\sum_{j=1,3,5}\{j^2\omega^2(a_j^2 + b_j^2) - U^2(a_j'^2 + b_j'^2)\} \quad (33)$$

$$\bar{P} = \tfrac{1}{2}Um_a(L)\sum_{j=1,3,5}\{j^2\omega^2(a_j^2 + b_j^2) + j\omega U(b_j a_j' - a_j b_j')\}, \quad (34)$$

where the values of a_j, b_j, a_j', b_j' are those at $x = L$.

We note that the mean total power $\bar{P}$ and the mean thrust $\bar{\theta}$ are the sums of the means for each frequency. The fluctuations within one period, however, are the result of an interplay between the various frequencies.

Rewriting equation (6) from Lighthill (1960), we find for the instantaneous thrust

$$\theta(t) = \tfrac{1}{2}\frac{1}{U}\int_0^L \frac{\partial H(x,t)}{\partial t} m_a(x)dx + \tfrac{1}{2}H(x,t)m_a(x)\Big|_{x=0}^{x=L}, \tag{35}$$

where H is defined by

$$H(x,t) = \frac{\partial h(x,t)^2}{\partial t} - U^2\left[\frac{\partial h(x,t)}{\partial x}\right]^2. \tag{36}$$

The time average of the integral in (35) vanishes and the second term yields (30). The second term becomes negative as well as positive during one half period. Our numerical calculations indicate that the first term cancels the strong fluctuations of the second term only for a small part.

The higher frequency terms contribute relatively very little to the thrust and total power according to our calculations. We therefore paid most attention to the first frequency terms; those with $j = 1$ in the above formulae. For the bending power per unit length, this term can be written as:

$$P_1(x,t) = \tfrac{1}{2}\omega f_1(x)M_1(x)\{\sin\omega[\sigma_1(x) - \mu_1(x)] - \sin\omega[2t - \sigma_1(x) - \mu_1(x)]\}. \tag{37}$$

This quantity fluctuates with a period of $T/2$. Its mean value is determined by the first term between the braces, it may be positive or negative depending on the phase difference between curvature f and bending moment M. The fluctuations are determined by the second term. P_1 changes its sign twice per $T/2$ (except when $\sigma_1 - \mu_1$ equals an odd multiple of $T/4$, then P_1 just touches zero). P_1 has a positive mean value if

$$kT < \sigma_1(x) - \mu_1(x) < (k + 1/2)T, \tag{38}$$

where k is any integer. The higher frequency contributions may influence the fluctuations of P_1, but for *any* periodic motion $P_1(x,t)$ is negative as well as positive in the course of one period, because P_1 is the product of two quantities, M and $\partial h''/\partial t$, which both change their signs periodically and generally not simultaneously. This means that at any cross section of the fish the power associated with the bending moment fluctuates around its local mean value, inevitably becoming negative or zero during part of the period.

For the power spent on fish plus water $P_2(x,t)$ (equation 14) expressions similar to those for P_1 can be derived. In the periodic case the time average $\bar{P}_2(x)$ is the mean differential power spent on the water, because the mean power spent on the body vanishes.

Recoil correction

We now must regard a crucial but rather inconvenient point: recoil. As mentioned before, the fish's motion must be such that the end conditions (6) are satisfied. Our functions h(x,t) do not satisfy these conditions for two main reasons: firstly, the lateral

motion h(x,t) as well as the mass functions $m_b(x)$ and $m_a(x)$ are not exact, but contain some errors. And, secondly, a real fish (such as saithe) is not a true slender body, hence the hydrodynamic forces computed on the basis of Lighthill's (1960) theory are not exact. Now we are faced with the problem of applying some sort of recoil correction to h(x,t) to make it satisfy the conditions (26) for the periodic case. There are many ways in which this could be done. We use one that is relatively simple, but not necessarily the best. We allow a certain amount of stiff motion A(t) + xB(t) to be added to h(x,t). In this manner the curvature f(x,t) is not affected. This stiff motion is represented by:

$$A(t) + xB(t) = \sum_{j=1,3,5} \{(r_{1j} + xr_{2j})\cos\omega t + (r_{3j} + xr_{4j})\sin\omega t\}. \tag{39}$$

For this motion we obtain, in analogy with (24):

$$\left.\begin{aligned} p_j''(x) &= -j^2\omega^2\{m_a(x) + m_b(x)\}(r_{1j} + xr_{2j}) + j\omega U\{2m_a(x)r_{4j} \\ &\qquad + m_a'(x)(r_{3j} + xr_{4j})\} + U^2 m_a'(x)r_{2j}, \\ q_j''(x) &= -j^2\omega^2\{m_a(x) + m_b(x)\}(r_{3j} + xr_{4j}) - j\omega U\{2m_a(x)r_{2j} \\ &\qquad + m_a'(x)(r_{1j} + xr_{2j})\} + U^2 m_a'(x)r_{4j} \end{aligned}\right\} \tag{40}$$

for j = 1, 3, 5. After integrating twice, we get:

$$\left.\begin{aligned} p_j'(L) &= +C_1 r_{1j} + C_2 r_{3j} + C_3 r_{2j} + C_4 r_{4j}, \\ q_j'(L) &= -C_2 r_{1j} + C_1 r_{3j} - C_4 r_{2j} + C_3 r_{4j}, \\ p_j(L) &= +C_5 r_{1j} + C_6 r_{3j} + C_7 r_{2j} + C_8 r_{4j}, \\ q_j(L) &= -C_6 r_{1j} + C_5 r_{3j} - C_8 r_{2j} + C_7 r_{4j}. \end{aligned}\right\} \tag{41}$$

The coefficients C_1 through C_8 can be computed from the functions $m_a(x)$ and $m_b(x)$ by numerical integration

$$\left.\begin{aligned} C_1 &= -j^2\omega^2 \textstyle\int_0^L \{m_a(x) + m_b(x)\}dx \\ C_2 &= j\omega U m_a(L) \\ C_3 &= -j^2\omega^2 \textstyle\int_0^L \{m_a(x) + m_b(x)\}x dx + U m_a(L) \\ C_4 &= j\omega U \{\textstyle\int_0^L m_a(x)dx + L m_a(L)\} \\ C_5 &= -j^2\omega^2 \textstyle\int_0^L \int_0^{x'} \{m_a(x) + m_b(x)\}dx dx' \\ C_6 &= j\omega U \textstyle\int_0^L m_a(x)dx \\ C_7 &= -j^2\omega^2 [\textstyle\int_0^L \int_0^{x'} \{m_a(x) + m_b(x)\}x dx dx' + U^2 \int_0^L m_a(x)dx] \\ C_8 &= j\omega U \{\textstyle\int_0^L \int_0^{x'} m_a(x)dx dx' + \int_0^L m_a(x)x dx\}. \end{aligned}\right\} \tag{42}$$

We proceed as follows. First we solve equations (7) and (8) for M''(x,t) using the original h(x,t) as derived from the film sequences. By twice integrating (25) we obtain $p_j'(L)$, $q_j'(L)$, $p_j(L)$, $q_j(L)$. The values at x = 0 vanish automatically. We want to add the appropriate amount of stiff motion. (Here the linearity of the theory is crucial.) Then the equations (41) must be solved for r_{1j}, r_{2j}, r_{3j} and r_{4j} with the left-hand sides

set equal to minus the corresponding quantities obtained from h(x,t). We then add the resulting stiff motion (39) to h(x,t). A similar treatment of recoil is given by Lighthill (1970).

This concludes the description of the mathematical model. The numerical calculations are carried out by evaluating the integrands at 101 equidistant points, and applying the trapezium rule on each of the 100 segments. The computing programme are written in Basic and run on an HP 9835A computer.

Dimensionless quantities

We shall express the physical quantities in dimensionless form, because this makes it easier to compare cases differing in size or swimming speed. The resistance or drag D which the fish must overcome when moving forward is often expressed as:

$$D = \tfrac{1}{2}\varrho U^2 A_w C_D\,, \tag{43}$$

where C_D is the dimensionless drag coefficient, and A_w the wetted surface area of the fish. ϱ is the density of water and also the mean density of the fish. Similarly the thrust coefficient C_T is connected with the thrust θ:

$$\theta = \tfrac{1}{2}\varrho U^2 A_w C_T\,. \tag{44}$$

If the Reynolds number is high enough (so that viscous effects are restricted to a thin boundary layer on the body surface), C_D depends only on the body shape of the fish, not on absolute size or speed. If thrust and drag are not equal in magnitude, then the fish accelerates or decelerates:

$$\theta - D = \varrho m_f \dot{U}\,, \tag{45}$$

where m_f is the fish's volume. From this follows:

$$C_T - C_D = \frac{m_f}{\tfrac{1}{2}A_w L}\,\frac{\dot{U}L}{U^2} = s\beta. \tag{46}$$

The first factor is the dimensionless shape parameter s, and the second factor is the dimensionless acceleration parameter β (see Videler & Hess, 1984). Just as in that paper we shall use the time period T as a unit of time and the fish length L as a unit of length. Further we choose the mass of a volume L^3 of water as a mass unit. In these units we have: $L = 1$, $T = 1$, $\varrho = 1$ and $\omega = 2\pi$. To convert to conventional units, lengths must be multiplied by L, times by T, velocities by $L\,T^{-1}$, forces by $\varrho L^4 T^{-2}$, moments by $\varrho L^5 T^{-2}$, powers by $\varrho L^5 T^{-3}$, powers per unit length by $\varrho L^4 T^{-3}$, mass per unit length by ϱL^2, etc.

Body shape of saithe

Fig. 3A shows the dorsal and lateral views of a swimming saithe as drawn from ciné pictures. Fig. 3B presents graphs for the body mass distribution m_b and the hydrodynamic lateral added mass distribution m_a. All quantities are made dimensionless as outlined above. The cross-sectional shape of saithe was determined by measuring three specimens (length about 0·22 m each). Ciné pictures were used to determine the shape of the tail fin during regular swimming, and to verify that the other fins were

almost completely collapsed. The body mass per unit length $m_b(x)$ and the lateral added mass per unit length $m_a(x)$ were calculated by:

$$\left.\begin{aligned} m_b &= \tfrac{1}{4}\pi b h_1 \\ m_a &= \tfrac{1}{4}\pi h_2^2, \end{aligned}\right\} \qquad (47)$$

where b is the local body width, h_1 the local body height excluding fins and h_2 including fins. Both formulae are valid for elliptical sections. Lighthill (1970) showed that deviations from the calculated m_a values are likely to be small. After b, h_1, h_2 were determined at some 18 points, smooth functions $m_b(x)$ and $m_a(x)$ were obtained by interpolation with cubic splines.

Some relevant quantities are:

Height of tail fin at trailing edge	: 0·24 [L]	
Added mass at trailing edge	: $m_a(L)$	$= 0{\cdot}0452\ [L^2]$
Body volume	: m_f	$= 0{\cdot}0113\ [L^3]$
Wetted area	: A_w	$= 0{\cdot}401\ [L^2]$
Shape parameter, see (45)	: s	$= 0{\cdot}0564$
Reynolds number (Re)	: between 2×10^5 and 8×10^5	

We may well pose the question: how closely does a saithe resemble a slender body? One may think of slender-body theory as an approximate theory whose resolving power is limited to details in space which have about the size of the cross-sectional dimensions of the 'slender' body. In our case that means roughly one-quarter of the fish length, which is not very good. (For eel it would be about one-tenth, which is much better.) In slender-body theory the mean thrust and the mean total power depend only on what happens at the tail end, but the theory implies that what happens just ahead of the tail end is not very different. Here 'just ahead' may mean an area as large as the whole fish tail in saithe. However, the height, for instance, varies strongly along the tail. From this it is clear that the numerical results presented in this paper should be considered as approximate estimates rather than as precise quantitative predictions.

It is quite likely that slender-body theory over-estimates the hydrodynamic forces, especially at the tail. Firstly, as pointed out by Lighthill (1970), the effective lateral added mass is smaller if the body wave length is not very much (say, at least five times) greater than the body height. Secondly, the tail region of saithe is not slender, strictly speaking. The tailfin roughly resembles a triangular wing of aspect ratio 4 (Fig. 3A). For such a wing in steady flow the lift is over-predicted by a factor of 1·8 by slender-body (or rather slender-wing) theory (Lawrence, 1951). The only remedy would be to employ some kind of unsteady lifting-surface theory, but that would involve tremendous complications in comparison with Lighthill's (1960) elegant slender-body theory.

RESULTS AND DISCUSSION

The third and fifth frequencies (j = 3, 5 in the formulae) each contributed only about 1 % to the power and the thrust (Fig. 6). Therefore, we shall deal only with the

Table 1. *Some data and results, for first frequency contribution only*

Sequence	T (s)	U ($L\,T^{-1}$)	$C_T - C_D$	a (L)	Without recoil correction		Recoil correction nose		tail		$\bar{P}$ ($\varrho L^5 T^{-3}$)	$\bar{\theta}$ ($\varrho L^4 T^{-2}$)	η	C_T	C_D
					η	C_T	ampl (L)	ph (T)	ampl (L)	ph (T)					
S1	0·287	0·86	0·002	0·098	0·66	0·011	0·017	0·28	0·026	0·72	0·0020	0·0019	0·82	0·013	0·011
S2	0·446	0·81	−0·000	0·067	0·60	0·003	0·014	0·34	0·018	0·78	0·0009	0·0009	0·84	0·007	0·007
S3	0·374	0·79	0·002	0·088	0·63	0·010	0·020	0·31	0·024	0·75	0·0017	0·0017	0·80	0·014	0·012
S4	0·305	0·84	0·003	0·092	0·66	0·009	0·012	0·29	0·022	0·75	0·0017	0·0017	0·82	0·012	0·009
S5	0·188	0·67	0·018	0·101	0·72	0·034	0·018	0·23	0·024	0·67	0·0021	0·0024	0·79	0·027	0·009
S6	0·261	0·82	0·006	0·098	0·68	0·014	0·015	0·30	0·026	0·71	0·0019	0·0019	0·82	0·014	0·008
S7	0·272	0·80	0·004	0·095	0·68	0·012	0·011	0·30	0·024	0·73	0·0018	0·0019	0·82	0·015	0·011
S8	0·515	1·21	−0·004	0·078	0·04	0·000	0·031	0·33	0·047	0·72	0·0018	0·0011	0·75	0·004	0·008
S9	0·178	0·99	−0·004	0·075	0·63	0·005	0·017	0·27	0·027	0·69	0·0010	0·0009	0·85	0·004	0·008
S10	0·222	0·75	0·001	0·091	0·52	0·009	0·014	0·36	0·029	0·76	0·0016	0·0017	0·79	0·015	0·014
S11	0·206	0·70	0·006	0·077	0·69	0·015	0·008	0·20	0·020	0·70	0·0012	0·0014	0·80	0·014	0·008
S12	0·150	0·94	−0·003	0·064	0·18	0·000	0·010	0·46	0·017	0·81	0·0007	0·0006	0·84	0·004	0·007
S13	0·215	0·95	−0·002	0·059	(1·23)	−0·005	0·010	0·62	0·020	0·98	0·0003	0·0002	0·66	0·001	0·003
av	0·278	0·86	0·002	0·083	0·63	0·007	0·013	0·31	0·023	0·74	0·0014	0·0013	0·83	0·009	0·007

Notes: $C_T - C_D$ follows from the observed acceleration according to (46).
a, tailpoint amplitude; ampl, amplitude; ph, phase; av, average.
For further explanation see main text.

first frequency (j = 1). Table 1 lists some results for the 13 sequences and also for the 'average' saithe obtained by averaging the Fourier coefficients a_j and b_j from the 13 sequences (see Videler & Hess, 1984).

Obviously, the stiff-body motion added as a recoil correction was considerable in all cases. Let us first look at the situation before the recoil correction was applied. The mean total power $\bar{P}$ and the mean thrust θ have been computed according to (34) and (33), and from these follow the thrust coefficient C_T (44) and the Froude efficiency η (32). If we leave the four decelerating cases out, η varied between 0·52 and 0·72. For 'average' saithe $\eta = 0{\cdot}63$. These values are lower than the estimates made in the preceding paper (Videler & Hess, 1984). There we looked at the motion of the posterior part, in particular the quantities $h_1'(x)/h_1(x)$ and $\tau_1(x)$. In the present calculations the trailing edge values were used, which turn out to differ somewhat from the mean values over, say, the last 10% of the fish length. Although the latter calculations were carried out with greater precision, we believe the former estimates to be more realistic.

For a saithe moving with the U and h(x,t) as analysed from the film sequences, the hydrodynamic forces computed according to slender-body theory would be such that the end conditions (6), or (26), could not be satisfied. Theoretically, the fish could only move that way if additional external lateral forces were to act at the nose and tail

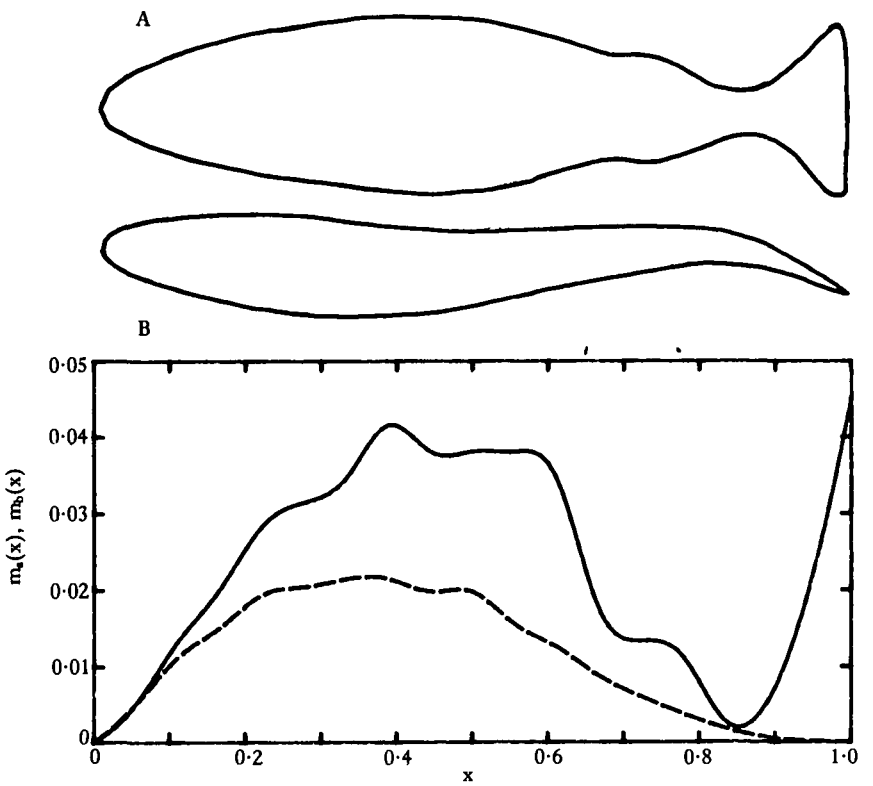

Fig. 3. (A) Shape of swimming saithe, lateral and dorsal views. (B) Distribution of body mass per unit length $m_b(x)$ (dashed curve) and lateral added mass per unit length $m_a(x)$ (drawn curve). (Unit: ϱL^2.)

ends. We computed these virtual forces. In all cases the external force at the tail end counteracted the computed hydrodynamic force, whereas the additional force at the nose end was much smaller. Let us take the case of 'average' saithe. The virtual force on the nose end had an amplitude 0·002 ($\varrho L^4 T^{-2}$) and reached its maximum at t = 0·33 (T). The virtual lateral force on the tail end had an amplitude 0·0063, and its maximum occurred at t = 0·90. Now, the lateral hydrodynamic force acting on the fish between x = 0·95 and x = 1·00 had an amplitude 0·0061 and reached its maximum at t = 0·36, that is 0·54 T earlier than the virtual force. Thus the computed hydrodynamic force on the last 5 % of the fish length was cancelled for a great part by the virtual force. This clearly shows that the saithe can only carry out its observed movement if the hydrodynamic force on the tail is much smaller in reality than as computed.

The stiff-body motion added as recoil correction is indicated in Table 1 by the values of its amplitude and phase at the nose and tail ends. Fig. 4 provides a comparison between the lateral motion before and after recoil correction for 'average' saithe. The amplitudes at nose and tail ends were hardly affected, but in between the 'corrected' amplitude was higher. The most significant change concerned the tail region, where $h_1'(x)$ was much reduced after the correction. The 'corrected' phase function $\tau_1(x)$ equalled −0·043 at the tailing edge rather than zero. The wave speed V ($= 1/\tau_1'$) was only marginally increased in the tail region, but its overall value was higher. Before recoil correction we have V = 1·04, U/V = 0·82, and after recoil correction V = 1·26, U/V = 0·68 over the posterior half of the fish.

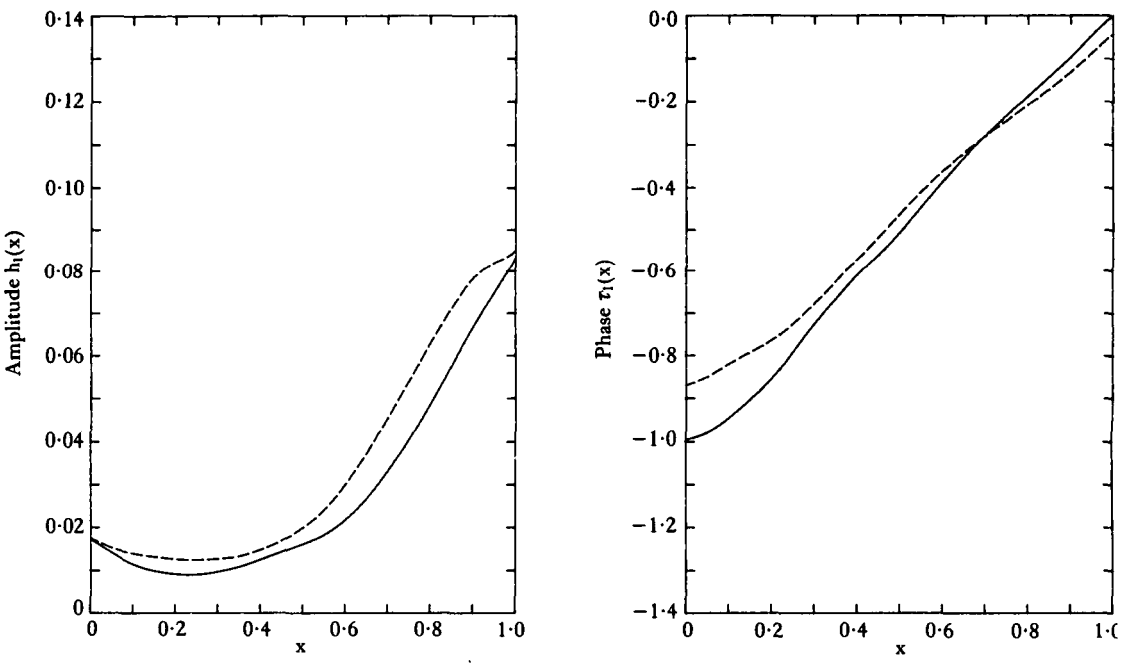

Fig. 4. Lateral motion of 'average' saithe before recoil correction (drawn curves) and after recoil correction (dashed curves). First frequency contribution only. Nose is at x = 0, tail point at x = 1. Left: amplitude functions $h_1(x)$ (unit: L). Right: phase functions $\tau_1(x)$ (unit: T).

Values for $\bar{P}$, $\bar{\theta}$, C_T and η after recoil correction are listed in Table 1. From the observed acceleration $C_T - C_D$ follows according to (46). This leads to the drag coefficient values in the last column of Table 1. The Froude efficiency η ranged from 0·65 to 0·84, or, if the four decelerating cases are left out, from 0·79 to 0·84. C_T varied between 0·001 for the decelerating S13 to 0·027 for the rather strongly accelerating S5. C_D varied between 0·003 and 0·014. For 'average' saithe we find $C_T = 0{\cdot}009$ and, as the average value for $C_T - C_D = 0{\cdot}002$, we estimate $C_D = 0{\cdot}007$. The mean total power $\bar{P}$ for 'average' saithe was 0·0014 ($\varrho L^5 T^{-3}$), which corresponds to about 0·7 W kg^{-1} body weight. (For S5 it is about 3·5 W kg^{-1}.)

The calculated thrust θ fluctuated during each half-period between zero and approximately twice its average value $\bar{\theta}$. For 'average' saithe $\theta = 0{\cdot}0013 \pm 0{\cdot}0011$. If the drag on the fish were constant, such thrust fluctuations would cause oscillations of the forward speed about its mean value U. According to (46) the fluctuations in $\dot{U}$ would have an amplitude:

$$\Delta\dot{U} = \frac{\Delta C_T U^2}{sL}. \tag{48}$$

This gives rise to relative speed fluctuations with amplitude:

$$\frac{\Delta U}{U} = \frac{\Delta C_T U}{s\omega L}, \tag{49}$$

where ΔC_T is the amplitude of the fluctuations in the thrust coefficient. For 'average' saithe (49) yielded about 2 %, and the maximum thrust occurred at $t \simeq -0{\cdot}24$ which was nearly simultaneous with the maximum bending moment, roughly when the tail point passes the plane $z = 0$. These fluctuations are somewhat stronger than those observed in the preceding paper (Videler & Hess, 1984). In the accelerating case S5 we find $\Delta U/U \simeq 5\,\%$, which agrees with the observed value. The computed instant of maximum thrust was at $t \simeq -0{\cdot}28$, whereas the kinematic data yielded $t \simeq -0{\cdot}20$.

Fig. 5 shows the amplitude $M_1(x)$ and the phase function $\mu_1(x)$ of the bending moment $M(x,t)$ for 'average' saithe. The bending moment was strongest in the central part of the fish body. The phase curve was nearly horizontal: $\mu_1(x) \simeq -0{\cdot}25$. This is by far the most striking result: the bending moment did not travel from head to tail as a wave but it reached its maximum value nearly simultaneously all along the body! The muscles on the right side of the body exerted their maximum contraction force at about the instant when the tail end, in its sweep from left to right, had reached the plane of symmetry ($z = 0$).

Fig. 6 shows the mean differential bending power $\bar{P}_1(x)$ and the mean differential power imparted to the water $\bar{P}_2(x)$. $\bar{P}_1$ was almost zero in the anterior part because the fish body hardly bends there, it reached a maximum in the central part around $x \simeq 0{\cdot}7$, and it was negative in the tail, which contains no muscles. Fig. 6 clearly shows that the power ($\bar{P}_1$) was generated in the region $0{\cdot}4 \lesssim x \lesssim 0{\cdot}9$ and spent on the water ($\bar{P}_2$) in the tail region $x \gtrsim 0{\cdot}85$. Considering the fish as a hydrodynamic propulsion machine: the central part of the fish body contains the motor and the tail serves as the propeller.

The fluctuation in the differential bending power $P_1(x,t)$ are not shown, but, as explained above, they were very strong. At $x \simeq 0{\cdot}65$, where the bending moment was

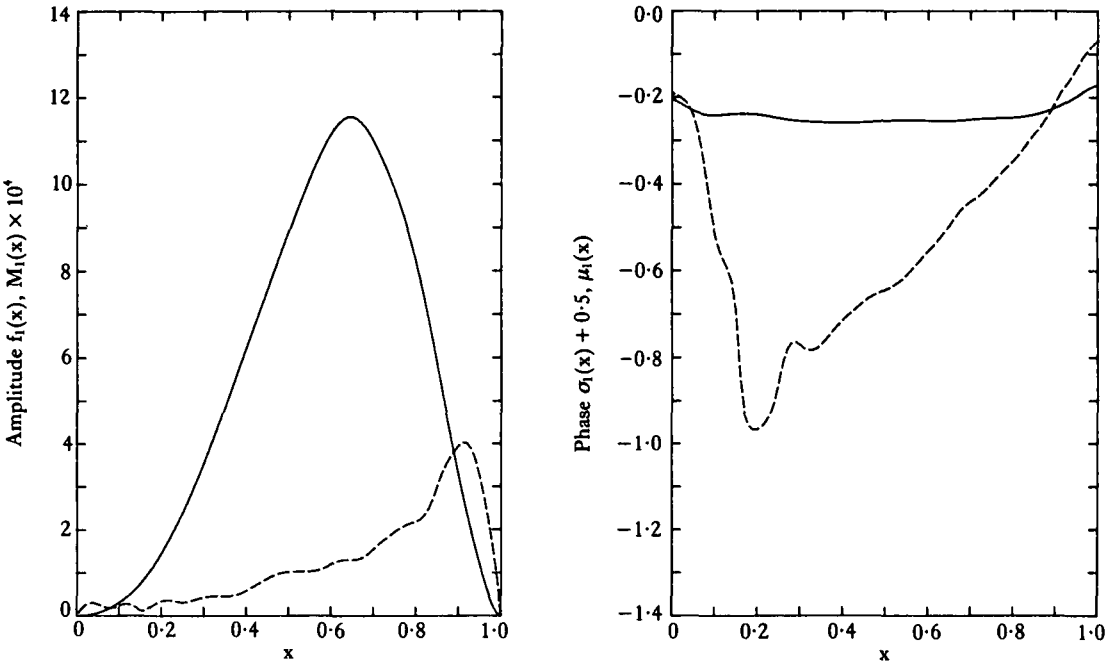

Fig. 5. Lateral body curvature (dashed curves) and lateral bending moment (drawn curves) for 'average' saithe. First frequency contribution only. Left: amplitude functions $f_1(x)$ (unit: L^{-1}) and $M_1(x) \times 10^4$ (unit: $\varrho L^5 T^{-2}$). Right: phase functions $\sigma_1(x) + 0{\cdot}5$ and $\mu_1(x)$ (unit: T). Because the body curvature found for $x \lesssim 0{\cdot}2$ is due to noise in the data rather than to real bending, the dashed phase curve has no physical meaning in this region.

greatest, P_1 fluctuated between zero and twice its mean value and at most other places the power became negative during part of each period. This implies that most of the lateral fish muscles used in swimming are periodically stretched while exerting a contracting force.

How accurate are the computed results presented here? Since the hydrodynamic forces are over-predicted (at least on the tail), the bending moment M, the differential bending power $\bar{P}_1$, and the thrust θ are likely to be over-predicted as well. We found, however, strong indications that the standing-wave character of the bending moment is not a spurious result but a real phenomenon. We have tried several ways to reduce the hydrodynamic force on the tail. We worked with a lower 'effective' tail height, or decreased the lateral added mass m_a as suggested by Lighthill's (1970) Fig. 2. Also we have employed a different curvature function f(x,t), which has its amplitude $f_1(x)$ increasing towards the trailing edge instead of decreasing. All these methods yield a reduced hydrodynamic tail force, a much smaller recoil correction and smaller values for $M_1(x)$, $\bar{P}_1(x)$, θ, C_T and hence C_D. But the curves for $\mu_1(x)$ remain approximately horizontal (with the possible exception of the last 10% of the fish length). None of these methods can be firmly justified theoretically, but their results firstly confirm our main finding that the bending moment does not move along the body as a running wave, and secondly indicate that the drag coefficient for saithe probably is $C_D \simeq 0{\cdot}005$.

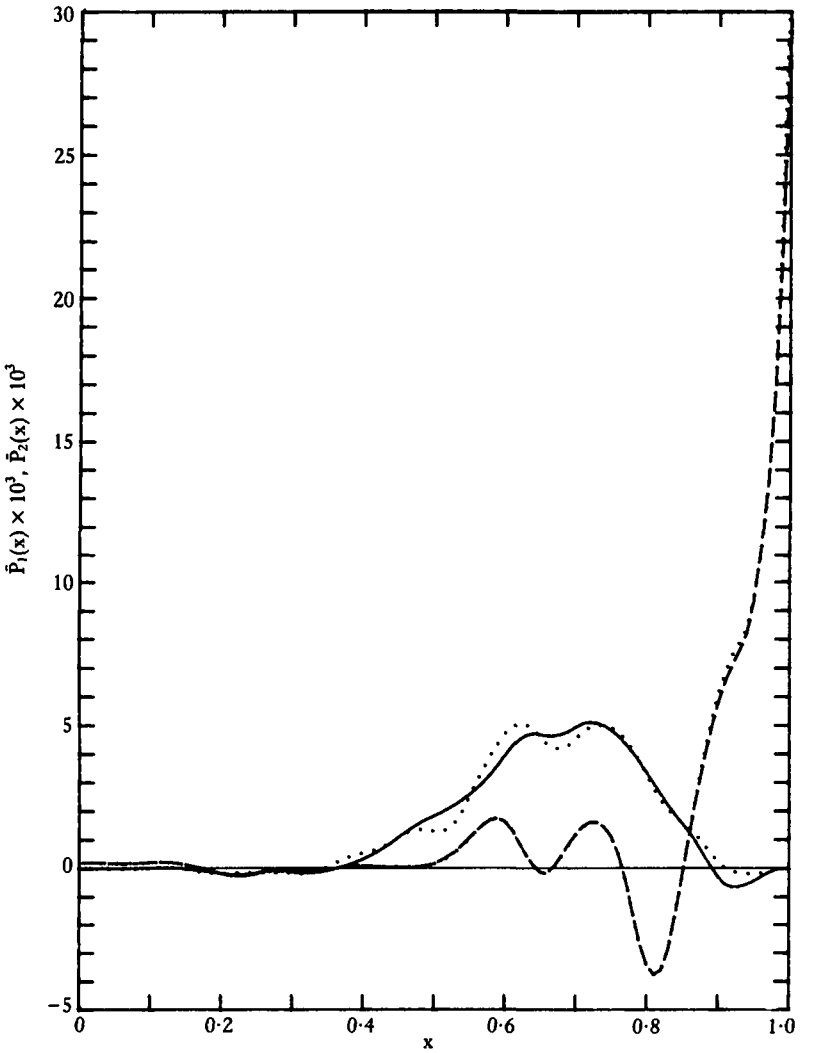

Fig. 6. Distribution of mean bending power per unit length $\bar{P}_1(x)$ and mean power spent on the water per unit length $\bar{P}_2(x)$ for 'average' saithe. (Unit: $\rho L^4 T^{-3}$). Drawn curve: $\bar{P}_1(x) \times 10^3$, first frequency contribution only. Dashed curve: $\bar{P}_2(x) \times 10^3$, first frequency contribution only. Dotted curves: $\bar{P}_1(x) \times 10^3$ and $\bar{P}_2(x) \times 10^3$, sum of first, third and fifth frequency contributions.

This is much lower than the high drag coefficient obtained from computed thrust by Lighthill (1971) for *Leuciscus*. For saithe we found no evidence to support his view 'that the viscous drag on the fish while it is swimming must for some reason be many times greater than that which would be associated with gliding motion'. We have not analysed film sequences of gliding saithe without lateral motion, which could have provided experimental values for C_D. For gliding cod (*Gadus morhua*), however, Videler (1981) found $C_D = 0{\cdot}015$, $0{\cdot}011$, $0{\cdot}011$ for one specimen in three gliding sequences.

Our findings are supported by preliminary results of a similar analysis of the swimming motion of eel (*Anguilla anguilla*). Hydrodynamically an eel behaves as a slender body to a good approximation. Indeed, the recoil corrections required for eel are much smaller than for saithe. The bending moment has the same character, although the phase function $\mu_1(x)$ in eel is not quite so constant as in saithe. The mean differential bending power $\bar{P}_1$ has roughly the same shape as in saithe, but the negative peak in the tail region is relatively more pronounced in eel. All these results are qualitatively similar to those presented here for saithe.

In deriving the major result, the 'standing wave' character of the bending moment, we started from a running wave of body curvature. And indeed, the swimming strategy of a fish might be to send waves of curvature along its body from head to tail. However, our findings indicate that a fish may well use the strategy of exerting bending forces simultaneously throughout its body, alternately using the muscles on the left side and on the right side. The running wave in its body shape is then the result of the interaction with the water flow. If this hypothesis is correct, the running wave should be absent if a fish starts from stand-still in water or moves in air, provided the fish produces the same muscle force. Our view is supported by Hertel's (1963) Fig. 169 of a trout starting and swimming, and also by Fig. 2 of Weihs (1973) of a trout accelerating from stand-still.

The use of lateral muscles in swimming

The results of our dynamic analysis provide new insight into the function of the lateral muscles for swimming. We shall first give a short description of the relevant structures of saithe and then discuss the implications of our findings with respect to muscle function.

Mechanically important parts of the locomotory apparatus used for continuous swimming include the vertical septum, and left and right lateral muscles, surrounded by the skin and the tailblade. The anatomy of these structures closely resembles that for cod, which is described by Wardle & Videler (1980) and Videler (1981). The vertical septum between the back of the head and the tailblade divides the body into two lateral halves. It is a sheet of collagenous fibres supported by the vertebral column. Mechanically the vertebral column can be regarded as an inextensible and incompressible flexible rod, easily bent in the horizontal plane. The connecting tissues between the vertebrae give the column self-restoring elastic properties (Symmons, 1979). The lateral muscles are metamerically arranged in myotomes separated by myosepts, both structures with a complicated geometry. The muscle fibres are attached to the myosepts and run approximately in the direction of the longitudinal body axis. Myosepts are attached to the vertical septum and at certain places to the skin. There is a thin layer of red aerobic muscle fibres on the outside of the myotomes just under the skin. The bulk of muscle fibres is white and works anaerobically. The lateral muscles are also firmly attached to the head and on the other end of the fish to the fin ray heads of the tailblade. From just behind the head (at $x \simeq 0{\cdot}2$) to the position of the anus (at $x \simeq 0{\cdot}45$) the ventral part of the fish contains the abdominal cavity. A thin layer of lateral muscles supported by ribs surrounds this cavity, and the lateral bending is restricted in this region. From the anus to the caudal end of the body the myotomes are bilaterally and dorsoventrally symmetrical.

The skin is a strong structure of layers of collagenous fibres in criss-cross arrangement (Videler, 1975). It is attached to the head and to the vertical septum along the dorsal and ventral rim and it inserts firmly on to the fin ray heads of the tailblade. The structure of the joints between the fin rays of the tailfin and the caudal peduncle allows the fish to keep the bending properties of the tailblade under muscular control. Details were given by McCutchen (1970) and Videler (1977, 1981). The curvature of the tailblade will be the result of elastic properties of the fin rays, controlled by intrinsic musculature in the peduncle and by lateral musculature *via* the skin, in interaction with bending forces exerted by the water.

The body curvature is connected with variations in length of the muscle fibres on either side of the septum. In our frame of reference, a positive curvature means that the fibres on the right side are shorter than their resting length, and those on the left side longer; for negative curvature it is the other way around. A positive bending moment implies that the muscles on the right side exert a contraction force and those on the left side are passive or exert a smaller contraction force. We simplify our line of reasoning by making the assumption that all the contraction forces are exerted by fibres lying at a distance from the septum $d(x) = \frac{1}{2}b(x)$ where b is the lateral thickness. This is approximately where the red muscle fibres are situated, and the simplified situation may not be too unrealistic during swimming at cruising speeds when most of the bending moment is generated by the red muscles. However, our assumption mainly serves as an instructive device.

The relative length change $\Delta l/l$ of the chosen fibres on the right side of the fish follows from the curvature h'':

$$\lambda_d(x,t) = -\frac{\Delta l}{l} = h''(x,t)d(x), \tag{50}$$

where λ_d is the relative shortening of the fibres. On the left side of the fish $\Delta l/l$ has the opposite sign. If the bending moment is generated by forces in the chosen fibres then the force $F_d(x,t)$ follows from

$$F_d(x,t) = M(x,t)/d(x)\,. \tag{51}$$

If M is positive then the contraction force F_d is exerted by the fibres on the right side, if M is negative then the contraction force $-F_d$ is exerted by the left-side muscles. The power produced by the hypothetical muscle fibres per unit length is given by:

$$F_d(x,t)\frac{\partial}{\partial t}\lambda_d(x,t) = M(x,t)\frac{\partial}{\partial t}h''(x,t) = P_l(x,t). \tag{52}$$

In Fig. 7 the functions F_d, λ_d and $\frac{\partial}{\partial t}\lambda_d$ are plotted as a function of time during one period for several cross sections along the fish body: $x = 0{\cdot}1(0{\cdot}1)0{\cdot}9$. At the nose and tail points ($x = 0$, $x = 1$) both F_d and λ_d vanish. The relative fibre length shortening $\lambda_d(x,t)$ is represented by the dashed curves. The extreme values reached are plus and minus 6%. In the tail region ($x = 0{\cdot}9$) the curvature is large (Fig. 5) but the body thickness is small, and λ_d varies between plus and minus 4%. The curve at $x = 0{\cdot}1$ is probably caused by noise in the kinematic data, since the fish's head is rigid. The contraction force $F_d(x,t)$ is represented by the drawn curves. It does not become very

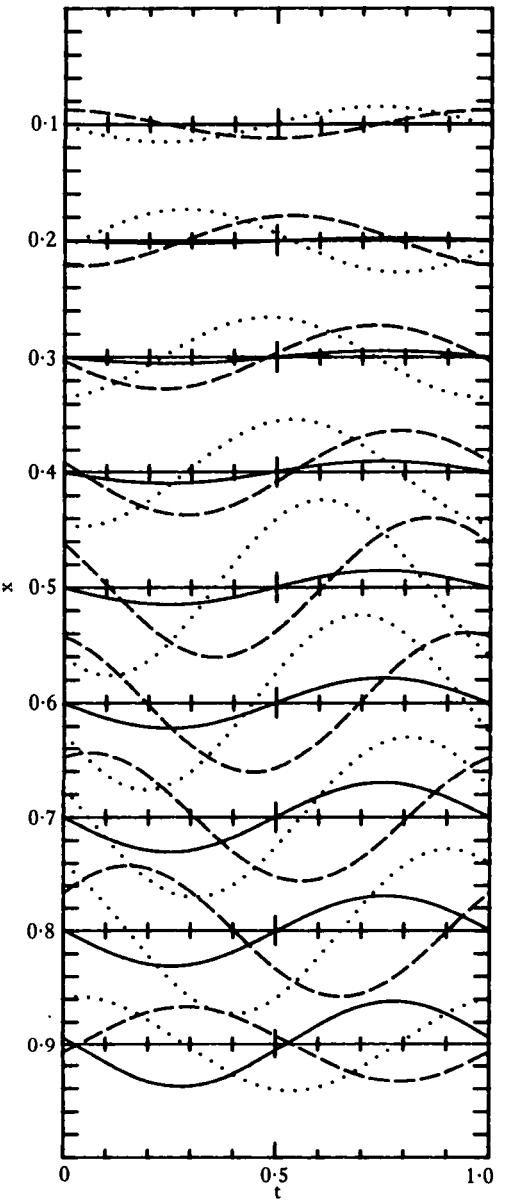

Fig. 7. Contraction force, relative length change and contraction speed in outer fibres (see main text for explanation) during one complete period at nine different sections of 'average' saithe. First frequency contribution only. Numbers at left indicate x-positions of sections. At x = 0 (nose) and x = 1 (tailpoint) all curves vanish. Drawn curves: contraction force in outer fibres, if positive then on the right side, if negative then on the left side. One vertical division equals $0{\cdot}02\,\varrho L^4 T^{-2}$. Dashed curves: relative shortening of outer fibres, if positive then the right-side fibres are shortened and the left-side fibres are lengthened. One vertical division equals 0·02 (= 2% length change). Dotted curves: contraction speed (that is the rate of change of relative shortening), if positive then the right-side fibres shorten. One vertical division equals $0{\cdot}1\,T^{-1}$. The bending power $P_1(x,t)$ at each section is obtained by multiplying the drawn curve by the dotted curve.

small in the tail region like the bending moment does, because d(x) is very small here. Let us now look at what happens in the region where the amplitude $M_1(x)$ and also the mean differential bending power $\bar{P}_1(x)$ are maximal: at $x = 0{\cdot}6$ or $x = 0{\cdot}7$. Between the instants $t = 0{\cdot}5$ and $t = 1$, F_d (drawn curves) is positive and the right-side fibres exert a contraction force. The right-side fibres shorten (see dashed curves) and reach their neutral length more or less when F_d is maximal. The contraction speed (stippled curves) reaches its maximum nearly at the same instant. Hence, the contraction force and the contraction speed have nearly the same phase. The power output (determined by the product of stippled curve and solid curve) is positive during almost the complete half period. Between $t = 0$ and $t = 0{\cdot}5$, F_d is negative, which means that the left-side fibres exert a positive contraction force $-F_d$. The right-side fibres lengthen (dashed curve falls), hence the left-side fibres contract. The drawn curve and the stippled curve also have the same sign during most of this half period. Therefore the power output is nearly always positive. At $x = 0{\cdot}6$, $P_1(x,t)$ is negative only for $0{\cdot}45 \lesssim t \lesssim 0{\cdot}50$ and $0{\cdot}95 \lesssim x \lesssim 1{\cdot}00$.

In the tail region the situation is completely different. Take the section at $x = 0{\cdot}9$. For $0{\cdot}53 \lesssim t \lesssim 1{\cdot}03$, $F_d(x,t)$ is positive, but the right-side fibres first lengthen and then shorten. The time intervals with positive power output and with negative power output are equally important. The mean differential power output $\bar{P}_1(x)$ nearly vanishes here. This part of the fish acts very much like an elastic element; the bending moment is greatest when the right side is stretched maximally. This behaviour agrees with the fact that the tail region does not contain muscles.

The opposite situation (resembling 'negative elasticity') is found at $x = 0{\cdot}4$. Here the bending moment is greatest when the right side is shortened maximally. The drawn curve and the stippled curve have the same sign during about half of the period, and the mean power output nearly vanishes (Fig. 6).

The sections at $x = 0{\cdot}5$ and $x = 0{\cdot}8$ are intermediate cases. At $x = 0{\cdot}8$, the contraction speed lags behind the contraction force, and at $x = 0{\cdot}4$, it runs ahead of the contraction force. When the right side at $x = 0{\cdot}8$ begins to exert a contraction force ($t \simeq 0{\cdot}5$) then the right-side fibres first go on lengthening (stippled curve is negative) and only at $t \simeq 0{\cdot}65$ do they begin to shorten.

Our analysis indicates that the muscles at $x \simeq 0{\cdot}65$ are used most efficiently with regard to energy output, contraction force and contraction speed being in phase. At cross sections such as those at $x = 0{\cdot}5$ and $x = 0{\cdot}8$ there is also a considerable contraction force, but it is not in phase with the contraction speed. At $x = 0{\cdot}4$ and $x = 0{\cdot}9$ the mean power output nearly vanishes.

Fig. 7 clearly shows how the running wave of body deformation together with the standing wave of the bending moment cause a phase difference between contraction speed and contraction force which varies systematically along the body from head to tail. Roughly speaking, when the muscles exert a maximum contraction force ($t \simeq 0{\cdot}75$ for the right side and $t \simeq 0{\cdot}25$ for the left side) then the muscle fibres in the muscular part of the tail from just behind the abdominal cavity to about half-way to the last unpaired fins ($0{\cdot}5 \lesssim x \lesssim 0{\cdot}7$) are close to their neutral length and are shortening at maximum speed. In the anterior part, around the abdominal cavity $0{\cdot}3 \lesssim x \lesssim 0{\cdot}5$), the fibres are maximally shortened at about that instant. In the caudal peduncle ($0{\cdot}8 \lesssim x \lesssim 0{\cdot}9$) the maximum force is generated just after the fibres are

maximally stretched. In this region a substantial part of the bending moment is probably due to elastic structures. Indeed, there are no lateral muscles in the tail beyond $x \simeq 0{\cdot}9$. Fig. 7 confirms that the section at $x = 0{\cdot}9$ shows a purely elastic behaviour.

The systematic differences in the use of lateral muscles along the body lead one to expect physiological or morphological adaptations to the different ways of contraction. There are no experimental indications as yet of such physiological differences between muscle fibres. The shape of the myotomes varies along the body but it is still not clear how this is related to our results.

Our analysis predicts that the muscle fibres on one side of the fish are simultaneously active. Consequently we expect myograms to occur simultaneously all along one side of the body. Such patterns have been found experimentally, and indeed Blight (1977) suggests that the running waves of lateral bending can be produced by 'alternations of tension development from side to side'. Blight (1976) finds instantaneous myograms along one side of swimming palmate newt larvae (*Triturus helveticus*) and in the same paper presents myogram patterns along the body of a swimming tench (*Tinca tinca*). His Fig. 4 indicates that the maximum muscle activity along the right side of the body occurs when the tail tip crosses the plane of symmetry from left to right, which agrees with our results. There is a small time delay between the muscle activity in the anterior and posterior part, the ending of the activity of the muscles just behind the head coincides with the beginning of activity in the caudal peduncle. The velocity of the wave of contraction is half as fast as the velocity of the wave of curvature. Grillner & Kashin (1976) find the wave of electric activity in the eel to be slower than the mechanical wave of bending. Kashin, Feldman & Orlovsky (1979) provide electromyographical evidence for a constant time lag between activation of anterior and posterior red muscles of the carp during sustained swimming and for simultaneous activation of homolateral segments during bursts of fast swimming. The above myographic data support our view of the use of lateral muscles in swimming.

This work is sponsored by the Foundation for Fundamental Biological Research (BION), which is subsidized by the Netherlands Organization for the Advancement of Pure Research (ZWO).

REFERENCES

BLIGHT, A. R. (1976). Undulatory swimming with and without waves of contraction. *Nature, Lond.* **264**, 352–354.

BLIGHT, A. R. (1977). The muscular control of vertebrate swimming movements. *Biol. Rev.* **52**, 181–218.

GRILLNER, S. & KASHIN, S. (1976). On the generation and performance of swimming in fish. In *Neural Control of Locomotion*, (eds R. M. Herman, S. Grillner, P. S. G. Stein & D. G. Stuart), pp. 181–201. New York: Plenum Press.

HERTEL, H. (1963). *Struktur, Form, Bewegung*. Mainz: Krausskopf.

KASHIN, S. M., FELDMAN, A. G. & ORLOVSKY, G. N. (1979). Different modes of swimming of the carp, *Cyprinus carpio* L. *J. Fish Biol.* **14**, 403–405.

LAWRENCE, H. R. (1951). The lift distribution on low aspect ratio wings at subsonic speeds. *J. aeronautical Sci.* **18**, 683–695.

LIGHTHILL, M. J. (1960). Note on the swimming of slender fish. *J. Fluid Mech.* **9**, 305–317.

LIGHTHILL, M. J. (1970). Aquatic animal propulsion of high hydrodynamic efficiency. *J. Fluid Mech.* **44**, 265–300.

LIGHTHILL, M. J. (1971). Large-amplitude elongated-body theory of fish locomotion. *Proc. R. Soc. B* **179**, 125–138.

MCCUTCHEN, C. W. (1970). The trout tail fin: A selfcambering hydrofoil. *J. Biomech.* **3(3)**, 271–281.

NEWMAN, J. N. & WU, T. Y. (1972). A generalized slender-body theory for fish-like forms. *J. Fluid Mech.* **57**, 673–693.

SYMMONS, S. (1979). Notochordal and elastic components of the axial skeleton of fish and their function in locomotion. *J. Zool., Lond.* **189**, 157–206.

VIDELER, J. J. (1975). On the interrelationships between morphology and movement in the tail of the cichlid fish *Tilapia nilotica* (L.). *Neth. J. Zool.* **25**, 143–194.

VIDELER, J. J. (1977). Mechanical properties of fish tail joints. *Fortschr. Zool.* **28**, 465–484.

VIDELER, J. J. (1981). Swimming movements, body structure and propulsion in Cod *Gadus morhua*. *Symp. Zool. Soc., Lond.* **48**, 1–27.

VIDELER, J. J. & HESS, F. (1984). Fast continuous swimming of two pelagic predators, saithe (*Pollachius virens*) and mackerel (*Scomber scombrus*): a kinematic analysis. *J. exp. Biol.* **109**, 209–228.

WARDLE, C. S. & VIDELER, J. J. (1980). Fish swimming. In *Aspects of Animal Movement*, (eds H. T. Elder & E. R. Trueman). *Soc. exp. Biol. Sem.* **5**, 125–150. Cambridge: Cambridge University Press.

WEIHS, D. (1973). The mechanism of rapid starting of slender fish. *Biorheology* **10**, 343–350.

WU, T. Y. (1971). Hydromechanics of Swimming Fishes and Cetaceans. *Adv. appl. Math.* **11**, 1–63.